



Tomatoes Are Red: The Perception of Achromatic Objects Elicits Retrieval of Associated Color Knowledge

Atsuko Takashima¹, Francesca Carota^{1,2}, Vincent Schoots^{1,3},
Alexandra Redmann³, Janneke Jehee¹, and Peter Indefrey^{1,2,3}

Abstract

■ When preparing to name an object, semantic knowledge about the object and its attributes is activated, including perceptual properties. It is unclear, however, whether semantic attribute activation contributes to lexical access or is a consequence of activating a concept irrespective of whether that concept is to be named or not. In this study, we measured neural responses using fMRI while participants named objects that are typically green or red, presented in black line drawings. Furthermore, participants underwent two other tasks with the same objects, color naming and semantic judgment, to see if the activation pattern we observe during picture naming is (a) similar to that of a task that requires accessing the color attribute and

(b) distinct from that of a task that requires accessing the concept but not its name or color. We used representational similarity analysis to detect brain areas that show similar patterns within the same color category, but show different patterns across the two color categories. In all three tasks, activation in the bilateral fusiform gyri (“Human V4”) correlated with a representational model encoding the red–green distinction weighted by the importance of color feature for the different objects. This result suggests that when seeing objects whose color attribute is highly diagnostic, color knowledge about the objects is retrieved irrespective of whether the color or the object itself have to be named. ■

INTRODUCTION

In speech production, a word in the mental lexicon needs to be activated based on the meaning or concept the speaker wants to express. Language production models differ with respect to their assumptions about how our knowledge about concepts is represented and how it is linked to the stored lexical representations. Some models (“feature list models,” e.g., Bierwisch & Schreuder, 1992; Jackendoff, 1990; Goldman, 1975) assume decompositional conceptual representations in which concepts (e.g., MOTHER) are the sum of their attributes or features (e.g., FEMALE and PARENT). Such features are, therefore, directly linked to the word “mother” in the lexicon. In contrast, the word production model of Levelt and colleagues (Levelt, Roelofs, & Meyer, 1999; Roelofs, 1992, 1993, 1997; Levelt, 1989) adopts a nondecompositional account of conceptual representations (“semantic network models,” e.g., Collins & Loftus, 1975) and assumes that only a node for the whole concept is linked to the corresponding lexical entry.

A question that has not been addressed by word production models so far is how much conceptual information is used for lexical access. A lower limit is given by the

need to select a specific word among all lexical entries. To select a specific word, the conceptual information that is used to access the lexicon must be sufficiently detailed to activate one word more strongly than all others. An upper limit is given by the total amount of available information about a given concept. Consider the case of naming a monochromatic picture of a banana. As participants normally have no problem recognizing the banana in such a picture and responding “banana,” the shape information alone seems to be sufficient to select the correct word. Hence, it could be that only the shape attribute is used to activate the lexical entry “banana.” Alternatively, the shape attribute might activate the whole concept BANANA, which in turn activates the lexical entry “banana.” In this case, some or all other information linked to the concept BANANA, such as its typical color, where this fruit grows, and what it costs in the supermarket, could be activated.

Intuitively, it seems not very plausible that all kinds of conceptual information (e.g., where bananas grow) should be used for lexical access in a simple picture naming task. Electrophysiological evidence indeed suggests that this is not the case. Abdel Rahman and Sommer (2003) used a combined lateralized readiness potential and N200-no-go response paradigm to assess the relative timing of the availability of semantic and phonological information in a two-choice/go/no-go picture naming task. They manipulated the kind of semantic information

¹Donders Institute for Brain, Cognition and Behaviour, Radboud University, Nijmegen, The Netherlands, ²Max Planck Institute for Psycholinguistics, Nijmegen, The Netherlands, ³Heinrich Heine University Düsseldorf, Germany

participants had to use for their response. In an “easy” condition, they were asked to decide between “small” and “large” real life size of depicted animals. In a “hard” condition, they were asked about the diet of the animals (“herbivore” or “carnivore”). They were able to show that the diet information was available later than the size information, but, crucially, this later availability did not delay the availability of phonological information about the name of the animal. Hence, the conceptual diet information could not have been used for accessing the lexical entry of the animal’s name.

Whereas the assumption that all available conceptual information is used for lexical access can be ruled out, it is still possible that some types of highly prominent conceptual features might become activated upon seeing a picture and play a functional role for lexical access. A good candidate for such a feature is color in the case of high color diagnostic (HCD) objects, that is, objects that are associated with a typical color. It has been shown that color information has an impact on the recognition of such objects (Tanaka & Presnell, 1999). If a picture of a banana is presented in yellow, it is recognized faster than if it is presented in an achromatic way or in an atypical color such as purple, indicating a better access to the object concept when the typical object color is present. In picture naming tasks, HCD objects are named faster when presented in their typical colors compared with when they are presented in grayscale format (e.g., Redmann, FitzPatrick, & Indefrey, 2019; Redmann, FitzPatrick, Hellwig, & Indefrey, 2014; see also the meta-analysis by Bramão, Reis, Petersson, & Faisca, 2011). Atypical color presentation simultaneously or just before picture presentation interferes with picture naming of a HCD object (Redmann et al., 2019). It is not clear, however, whether such effects on naming latencies arise at the stage of object recognition or reflect an influence of color information on lexical retrieval.

Furthermore, names of HCD objects elicit color Stroop effects (Dalrymple-Alford & Azkoul, 1972; Klein, 1964), implying that the color attribute must be retrieved from the concept activated by the name without actually seeing the color. The color Stroop effect is modulated by the strength of the association between the object name and the color, more strongly associated colors eliciting a stronger Stroop effect (Scheibe, Shaver, & Carrier, 1967). In principle, a higher association strength could be because of a stronger connection between the name of an object and the names of its corresponding color. It could also be because of heightened activation of the color concept evoked by the object’s name, especially when that color is very typical for that object. It is thus unclear whether the influence of association strength on the Stroop effect arises at a lexical or a conceptual level.

The color attribute provides a unique opportunity to study the neural correlates of attribute activation because of the existence of a neural substrate for color processing in the fusiform and lingual gyri (Human V4; Lueck et al.,

1989; Zeki, 1983). The color-sensitive cortex is activated when viewing HCD objects (Bramão, Faisca, Forkstam, Reis, & Petersson, 2010) and also when conceptual color knowledge is retrieved based on object names (Simmons et al., 2007; but see Chao & Martin, 1999, for the observation of distinct cortical regions for perceiving color and retrieving color knowledge). Internally generated color images have been found to activate areas that are active during actual color perception in people with grapheme color synaesthesia (van Leeuwen, Petersson, & Hagoort, 2010).

Those seminal studies have demonstrated brain activation patterns related to color processing even when colors are not perceptually present. The univariate analyses they employed, however, are agnostic about which colors are being activated. Recent advances in neuroimaging data analyses allow us to distinguish brain activation patterns when perceiving different colors (Bannert & Bartels, 2018; Seymour, Williams, & Rich, 2015; Brouwer & Heeger, 2009, 2013; Seymour, Clifford, Logothetis, & Bartels, 2010; Parkes, Marsman, Oxley, Goulermas, & Wuerger, 2009; Seymour, Clifford, Logothetis, & Bartels, 2009). In a comprehension study, Vandenbroucke, Fahrenfort, Meuwese, Scholte, and Lamme (2016) used a multivoxel pattern analysis technique to see if the brain shows color-specific patterns to HCD objects when the perceived colors of the objects were ambiguous. In their study, the objects that were either typically green or red were shown with a color that was in between red and green. The brain patterns in the visual areas V3 and V4 were classified as either red or green, corresponding to the typical color of the object. This is in line with behavioral findings that perceived colors are determined not solely by the wavelength of the light but also by our knowledge of the color of the objects (Mitterer & de Ruiter, 2008; Hansen, Olkkonen, Walter, & Gegenfurtner, 2006). For instance, the same hue color can be perceived as yellow when viewed on a banana, but as orange when viewed on a carrot.

There are different ways of applying multivariate pattern analysis to the brain data. One way is to train a classifier on two or more categories, and test whether the classifier can reliably categorize test trials from their brain activation pattern. Another approach is to search for brain areas that show a multivoxel activation pattern that resembles that of a model pattern (representational similarity analysis [RSA]; Carota, Nili, Pulvermüller, & Kriegeskorte, 2021; Nili et al., 2014; Kriegeskorte, Mur, & Bandettini, 2008). The latter approach compares the brain activation pattern of trials that can be grouped into specific categories to a theoretical space representing the categories. This can be applied for different categories of colors. If a part of the brain responds with a specific pattern to a given category, then within-category trials would show a similar pattern across trials but would be different from the patterns of the other categories. For instance, Bird and colleagues presented different hues of color

boxes between green and blue (Bird, Berens, Horner, & Franklin, 2014). Using the RSA approach, they were able to show that visual areas responded differently to blue boxes as compared with green boxes when they were perceived as blue or green, respectively. Taking this approach, one could test if the pattern of activation for typically green objects is different from that of typically red objects. The advantage of RSA is that it uses distance measures instead of a classifier to characterize the representational space, giving us the opportunity to model graded distance between the categories rather than binarizing it.

In this study, we applied the RSA approach to answer the question of whether we evoke typical color activation patterns in our brain during the viewing and naming of HCD objects. The participants were shown black line drawings of HCD objects while being scanned in the MRI scanner. In an object naming task, the participants were instructed to name the object covertly upon visual presentation of the object. To test if the relevance of color information for the task affected the color-related dissociation pattern, the participants underwent two other tasks with the same visual stimulation. In one task, the participants were instructed to covertly name the typical color of the object (color naming task), and in the other, the participants were instructed to covertly respond whether the object was “man-made” or “natural” (color agnostic semantic decision task). We reasoned that, if the color attribute would only be activated in the color naming task but not in the object naming or the semantic decision tasks, the activation of conceptual attributes such as color is limited to those attributes that are necessary for a given task. This result would suggest that lexical access in word production can take place based on a minimal set of attributes required to recognize a depicted object and to activate its concept, and that surface color would not necessarily be part of this minimal set. If, on the other hand, color activation would be found in all three tasks, this would suggest that (at least important) attributes are automatically co-activated with their object concepts, irrespective of whether the attribute information is relevant for a given task. If, finally, color activation was found for the two naming tasks but not for the semantic decision task, this would suggest that the activation of an attribute, that is, color, that is neither necessary for the task at hand nor automatically activated might depend on the retrieval of the name of the corresponding object or even have some functional role in retrieving the object name.

Considering the behavioral evidence discussed above that the association strength between an object name and its color may modulate the degree of activation of the color concept or the color name, we analyzed the color activation patterns by taking into account the strength of the color association as well as the importance of the color feature for our HCD objects. We reasoned that although the strength of the association might reflect

both word level and conceptual links between the (names of) the object and (the names) of their colors, the differential importance of its color for an object might be more indicative about color as an important conceptual property of the object.

METHODS

Participants

Given the estimated effect size of the study by Bannert and Bartels (2013) on the visual cortex decoding analysis to be $d = 1.25$, we calculated power based on a moderate effect size of 0.5 on the color knowledge activation using G*power (Faul, Erdfelder, Lang, & Buchner, 2007). This yielded a sample size of 27. With possible dropouts in mind, 32 healthy, right-handed participants (15 men, age mean = 21.8 years, range = 18–26 years) with normal or corrected-to-normal vision were recruited via the online registration system of Radboud University Nijmegen. They all reported to be without color blindness and without neurological or psychiatric diseases. All participants signed informed consent before inclusion, and the study was approved by the local ethics committee in line with the Declaration of Helsinki. Three participants decided to discontinue and were excluded, and an additional two participant data sets were excluded because of noncompliance with some of the tasks. The study is thus based on the data of 27 participants (12 men).

Materials

Five objects that are typically green (cactus, turtle, frog, crocodile, and tank) and five objects that are typically red (lobster, strawberry, cherry, tomato, and fire engine) were chosen, and for each object, three black line drawings depicting the objects from different angles were created.

Tasks

Object Naming Task

Participants were presented with black line drawings of the 10 objects, depicted with three different drawings of each object. Every run contained 100 trials where 10 objects were repeated 10 times each per run, in a pseudo-random order, repeated in different orders for the four separate runs. Three different exemplars of the objects were semirandomly distributed within and across runs. Stimulus order was optimized for the event-related design using graph theory (Brooks, 2012) and implemented in an adaptation of the MATLAB (The MathWorks) script used by Brooks (2012). Optimization ensured that within each scanner run, every stimulus was preceded at least once by every other stimulus and itself. Stimulus timing was optimized for detection efficiency by MATLAB scripts built from the materials suggested by Mumford (n.d.; <https://www.youtube.com/channel/UCZ7gF0zm35FwrFpDND6DWeA>

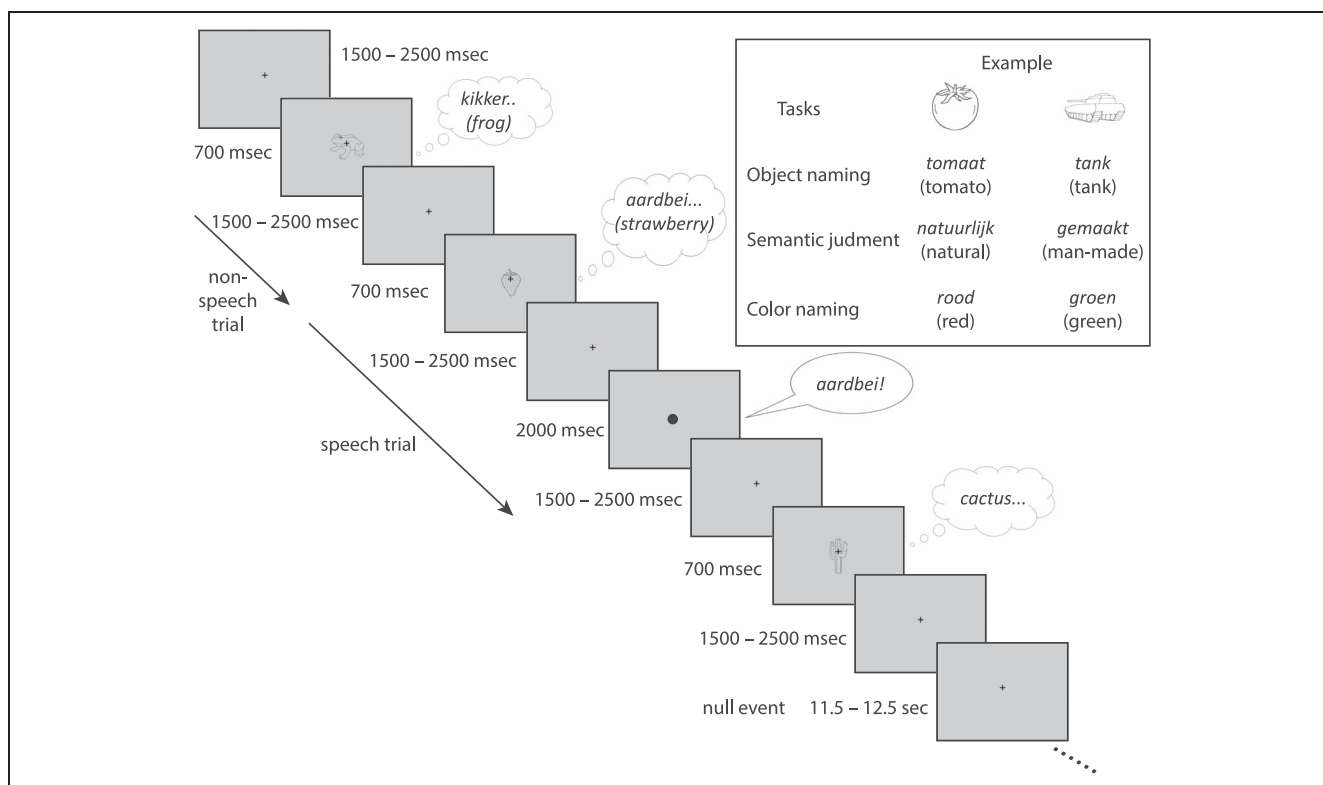


Figure 1. Object naming, semantic judgment, and color naming tasks. After every ITI of 1500–2500 msec, a line drawing picture appears on the center of the screen for 700 msec. Participants are instructed to name the object or the color covertly (object naming and color naming tasks, respectively), or to covertly assess whether the object is natural or man-made (semantic judgment task). In cases where a dot appears after the picture presentation, participants are instructed to make an overt response. Participants are also instructed to fixate on the center cross throughout the experiment. The figure shows timing of the trials during the three tasks, with example responses given during the object naming task.

/featured). Multiple lists of object presentation order were created following this rule, and for every participant and every run, a different list was used to avoid repetition in the order of appearance. During the scan, a black fixation-cross was presented in the center of a gray screen continuously, apart from when overt speech cues were given by turning the fixation-cross to a black dot (Figure 1). Participants were instructed to always fixate on the fixation cross (or the dot) throughout each run. For every trial, one of the objects would appear in the center of the screen for 700 msec and the participants were instructed to name the object covertly. For one eighth of all trials, after the picture offset with a delay between 1500 msec and 2500 msec, the fixation-cross turned into a black dot for 2000 msec. Participants were instructed to name the object overtly if this speech cue (dot) appeared on the screen. All trials were followed by an intertrial interval (ITI) that was jittered by sampling randomly from a homogeneous distribution of durations between 1500 msec and 2500 msec. Furthermore, null trials were inserted on random intervals after 2–16 trials, resulting in an average null trial occurrence of 11.1%. During the null trials, the fixation-cross remained on screen; their durations were sampled between 11.5 and 12.5 sec.

To observe test–retest reliability for this task, we performed two sessions of the object naming task (once in

Session 1 and again in Session 2), as this was the task of most interest and relevance for word production theories.

Semantic Judgment Task

For the semantic judgment task, 10 objects were presented 10 times each per run for four runs, as in the object naming task, but with different order lists such that the order of presentation and the ITI would be different from the other runs, also for the runs of the other tasks. Participants were instructed to name covertly whether the object was “gemaakt” (man-made) or “natuurlijk” (natural). If a dot followed the trial, the participants were instructed to make an overt response (say out aloud either “gemaakt” or “natuurlijk”).

Color Naming Task

Stimuli were the same as for the two tasks above, but were presented with a different order list for each of the four runs. In this task, there were also 100 trials in each run (10 objects × 10 times). In this task, the participants were instructed to name the typical color of the objects covertly. When cued with the dot, the participants were instructed to name the color out aloud.

Circle Task

In addition to the tasks involving picture presentations, we employed a baseline color processing task to define our ROI. In this task, green and red concentric circles of two brightness values (dark/light) were shown to the participants, similar to those presented in Bannert and Bartels (2013) but using only the colors red and green, which were equated for perceptual luminance (see below). The circles extended to 7.19 visual degrees from the central fixation dot, and moved inward or outward randomly on each trial with a velocity of 1°/sec for 2 sec. After each trial, there was an ITI of 1 sec. The stimuli were presented on an achromatic (gray) background. The task was to indicate via button press whether the motion was in the same or in the opposite direction from the previous trial (1-back task). The stimuli were presented in three runs, 32 mini-blocks per run, and four trials per mini-block. Each mini-block contained circles of the same hue/brightness.

Before scanning, the luminance values were adjusted individually using the minimal flicker paradigm (Kaiser, 1991). Both red and green were luminance-matched to the background luminance +10% or -10%, resulting in four types of stimuli (light and dark green, light and dark red).

Retinotopic Mapping

Ten runs of retinotopic mapping scans were acquired for a separate study and not analyzed for this study.

Questionnaire

At the end of Session 3 (see Figure 2 for the session structure), participants were asked to answer questions presented on the computer. The questionnaire included questions regarding the participants' associations with the 10 objects used in the experiment. The questions included the following (in Dutch):

1. How familiar are you with the object in your daily life? (Likert scale 1–7, 1 = *not familiar at all*, 7 = *very familiar*)

2. How much do you associate a specific color with this object? (Likert scale 1 = *can be associated with any color*, 7 = *this object is strongly associated with one color*)
3. How would you describe the object in terms of color and texture? (Open answer)
4. How strongly do you associate the object with the color green? (Likert scale 1 = *not at all*, 7 = *very strongly*)
5. How strongly do you associate the object with the color red? (Likert scale 1 = *not at all*, 7 = *very strongly*)

The responses to Questions 4 and 5 were used as ratings for the color association rating model used in the imaging data analyses.

Procedure

Participants came to the laboratory on three separate days (see Figure 2), scheduled 1–31 days apart (except for two participants, whose second and third sessions took place 50 and 86 days, and 102 and 161 days after the first session, respectively). During Session 1, participants performed two tasks in the MRI scanner. The first task was the object naming task, and the second was the semantic judgment task. The tasks were preceded by practice rounds with example trials using different pictures than those of the actual experiment. Participants could repeat the practice round until they felt confident with the task. Then four runs of the actual task followed with the scanner on. Thus, for each task, four runs of the same task followed the practice block(s). At the end of the session, an anatomical scan of the brain was collected. During Session 2, participants performed two tasks in the MRI scanner, first the object naming task and, then, the color naming task. The tasks were always preceded by a practice run, and there were four runs for each task. At the end of the session, an anatomical scan of the brain was collected. During Session 3, participants performed two tasks in the MRI scanner. The first task was the circle task, comprising of three runs. This was followed by 10 retinotopic mapping runs. At

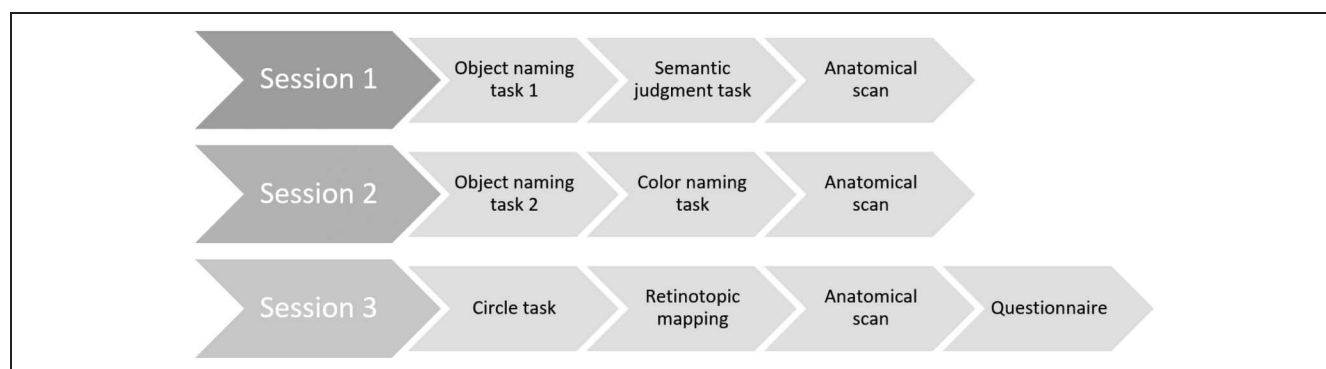


Figure 2. Study design and procedure.

the end of the scanning session, an anatomical scan of the brain was collected. The session ended with filling out questionnaires on the computer.

Data Acquisition

MRI data were recorded using a 3 T MR scanner (Skyra, Siemens Healthcare) and a 32-channel head coil. Whole-brain functional images were collected using a multi-echo multiband (accelerator factor of 3) T2*-weighted sequence: repetition time: 1510 msec; echo times (TE 1 = 14.20 msec, TE 2 = 36.36 msec, TE 3 = 58.52 msec), flip angle = 75°, field of view = 210 × 210 mm; 51 slices; voxel size = 2.5 × 2.5 × 2.5 mm. Participant's head was secured comfortably with a Tempur pillow to reduce motion as much as possible. In addition, T1-weighted anatomical scans at 1-mm isotropic resolution were acquired with repetition time = 2300 msec, TE = 3.03 msec, flip angle = 8°, and field of view = 256 × 256 × 192 mm.

Data Analysis

fMRI Data Preprocessing

Raw MRI Digital Imaging and Communication in Medicine (DICOM) files were first transferred to Neuroimaging Informatics Technology Initiative (NIFTI) format and stored in a Brain Imaging Data Structure using BIDScoin Version 2.1 (github.com/Donders-Institute/bidscoin). Subsequently, the NIFTI converted data were preprocessed using functions in SPM12 (www.fil.ion.ucl.ac.uk/spm/software/spm12/). The first echoes of each image were realigned to the first volume of each run, and the realignment parameters were applied to the other echoes of each data point. Multiple echo images were combined to one volume for each data point by using the first 30 volumes of each run to calculate the optimal weighting of the echoes for each voxel, and these weightings were applied to the rest of the functional images (Poser, Versluis, Hoogduin, & Norris, 2006). The 30 volumes used for echo weight calculations were then discarded. Multiple runs were then realigned to the first run for each task and resliced. Functional images were co-registered to the anatomical image acquired during the first session. The structural image acquired during the first session was segmented into gray matter, white matter, and cerebral spinal fluid compartments.

Circle Task

We first estimated voxel beta weights for the circle task using a general linear model (GLM) implemented in SPM12. We categorized the trials into eight conditions (light green inward move, light green outward move, dark green inward move, dark green outward move, light red inward move, light red outward move, dark red inward move, and dark red outward move). One GLM was constructed for all runs with these eight conditions in each

run together with six movement-related parameters per run derived from the preprocessing step as nuisance regressors. Parameter estimates for each condition per run was estimated in a participant native space. We used realigned, nonnormalized and unsmoothed data, which were co-registered with the T1 data of each participant. Stimulus onset time was set to the onset of each trial, its duration was set to 2 sec, and each trial was convolved with the canonical hemodynamic response function (HRF) provided by SPM12. A high-pass filter was implemented using a cutoff period of 128 sec to remove low-frequency effects from the time series. Applying the model to the data resulted in beta values for each of the eight stimulus conditions and for each individual voxel. To improve signal-to-noise ratio, two contrast images (one for green and one for red) were created per run by combining all four green conditions against the implicit baseline as one contrast and all red conditions against the implicit baseline as the other contrast for each run. This resulted in six contrast images (2 conditions × 3 runs).

Next, a whole-brain searchlight decoding classifier using The Decoding Toolbox (v3.999, <https://sites.google.com/site/tdtdecodingtoolbox/>) was carried out within each participant's gray matter mask. For every voxel, we selected all voxels in a sphere with a radius of 10 mm surrounding this voxel (voxel size 2.5 × 2.5 × 2.5 mm). Using a leave-one-run-out approach (i.e., train on two runs and test on one run, reciprocally), for each voxel, accuracy-chance values were calculated with the linear support vector machine (Hebart, Gørgen, & Haynes, 2015). The resulting accuracy-chance maps of each participant were then normalized to Montreal Neurological Institute (MNI) space using the normalization parameters estimated during the segmentation of the T1 image, and smoothed with 4-mm kernel FWHM. To test on the group level, a one-sample *t* test was performed on the normalized accuracy-chance maps. Areas that showed higher than chance level (thresholded at voxel level uncorrected $p < .05$) were interpreted as areas that disambiguated green from red colors (Figure 3). We took this very lenient threshold as the purpose of this task was to create the green/red distinguishing mask (green–red mask) for subsequent RSA analyses for the naming and judgment task data.

Naming and Judgment Tasks

For the naming and judgment tasks (color naming, object naming Session 1, object naming Session 2, semantic judgment), we first estimated contrast maps for each of the 10 objects and for each run per participant using a GLM implemented in SPM12 for each of the tasks separately. The design matrix for the GLM included three task-related regressors: The first regressor modeled the covertly named object of interest, the second regressor modeled all other objects, and the third regressor modeled overt speech. For example, in the object naming task, to create a beta map for the object “frog,” all trials pertaining

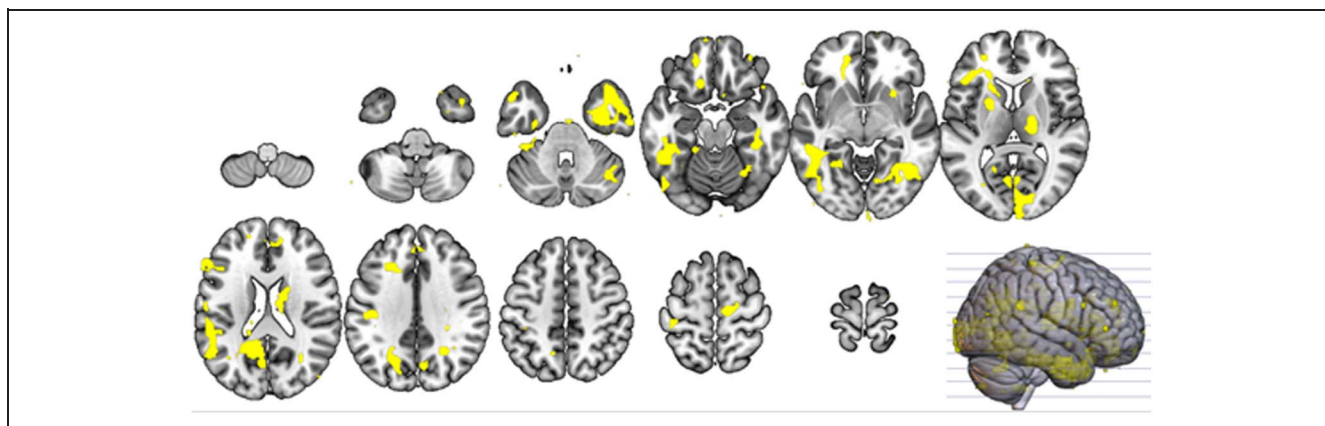


Figure 3. Green–red mask. Voxels above chance level for decoding green from red for the circle task, thresholded at voxel level uncorrected $p < .05$.

to “frog” were modeled in the first regressor, whereas the second regressor modeled for the remaining nine object trials, following the least squares single approach (Mumford, Davis, & Poldrack, 2014; Mumford, Turner, Ashby, & Poldrack, 2012), and the third modeled all the overt speech periods. Each covert naming event was set at the onset of the picture. For the speech trials, the onset was set at the appearance of the dot (speech cue) on the screen. Duration of the trials were set to 0 sec, which applies the default HRF curve for modeling the events. These explanatory variables were temporally convolved with the HRF provided by SPM12. Twenty-one motion-related regressors were added to the model to account for motion-related signal changes: 6 motion parameters derived from the realignment step mentioned above, 6 derivatives of the motion parameters, 6 squared values of the 6 derivative parameters, and 3 compartment-related regressors. Compartment-related regressors consisted of three time series: mean signal calculated within every volume for the white matter, cerebral spinal fluid, and out-of-brain area masks (a similar approach is explained in Verhagen, Dijkerman, Grol, & Toni, 2008). A high-pass filter was implemented using a cutoff period of 128 sec to remove low-frequency effects from the time series. This resulted in a beta map for the first regressor of each GLM, corresponding to the “object of interest.” For each object, the beta images of multiple runs were then averaged to create one beta map per object for each participant.

Next, a whole-brain searchlight multivariate RSA approach (Nili et al., 2014; Kriegeskorte et al., 2008) was carried out within the gray matter mask of each participant. For every voxel, we selected all voxels in a sphere of radius 10 mm surrounding this voxel (voxel size was $2.5 \times 2.5 \times 2.5$ mm) and created a vector of beta values (from the GLM analysis, see above) for that specific sphere. For each object pair, we then computed the Pearson correlation coefficient between the two vectors. A representational dissimilarity matrix (RDM) was subsequently created for every voxel by first calculating the correlation distance between the contrast maps of two objects (1 = the correlation

coefficient) and then entering these distances in a 10×10 matrix. For instance, the vectors with beta values for “turtle” and “fire engine” were compared for each sphere around the center voxel. If the pattern of the sphere vector was very dissimilar between the two objects, the center voxel would be assigned a higher score for this pair, and if the pattern was similar, the score would be lower for the turtle–fire engine pair. In this manner, we obtained a representational distance score for each pair of stimuli at every voxel within the gray matter mask. This representational distance between each pair yields a matrix (the data RDM), and this matrix can now be compared with other matrices, such as theoretically based model RDMs (color association rating and color feature importance; see Figure 4). These brain data RDMs were then correlated with the categorical RDM (model RDM) using Spearman’s rank correlation. The comparison yields an r statistic of every voxel comparing the data RDM and the model RDM.

We tested the brain data RDMs against two model RDMs. For the first color association rating model, we used the participant-specific color association ratings of each participant that they filled out in the questionnaire at the end of the experiment. To create the participant-specific model RDM between each pair of objects, we took the Euclidean distance of green association score (y axis) and red association score (x axis). For instance, if a participant responded green:7 and red:2 for frog, and green:1 and red:6 for lobster to the questions regarding the green-ness and red-ness associations (1 = no association, 7 = very strong association), the dissimilarity distance between frog and lobster would be calculated as the square root of $((7-1)^2 + (2-6)^2) = 7.2$ (Figure 4, top).

For the second model RDM, the color importance model, we took into account how important the color attribute was for a given concept. For some objects, the color attribute is more important for distinguishing them from otherwise similar objects (e.g., distinguishing lemon from lime) than it is for other objects (e.g., a car). We reasoned that color importance might modulate the degree of color activation. To test this, we designed a second

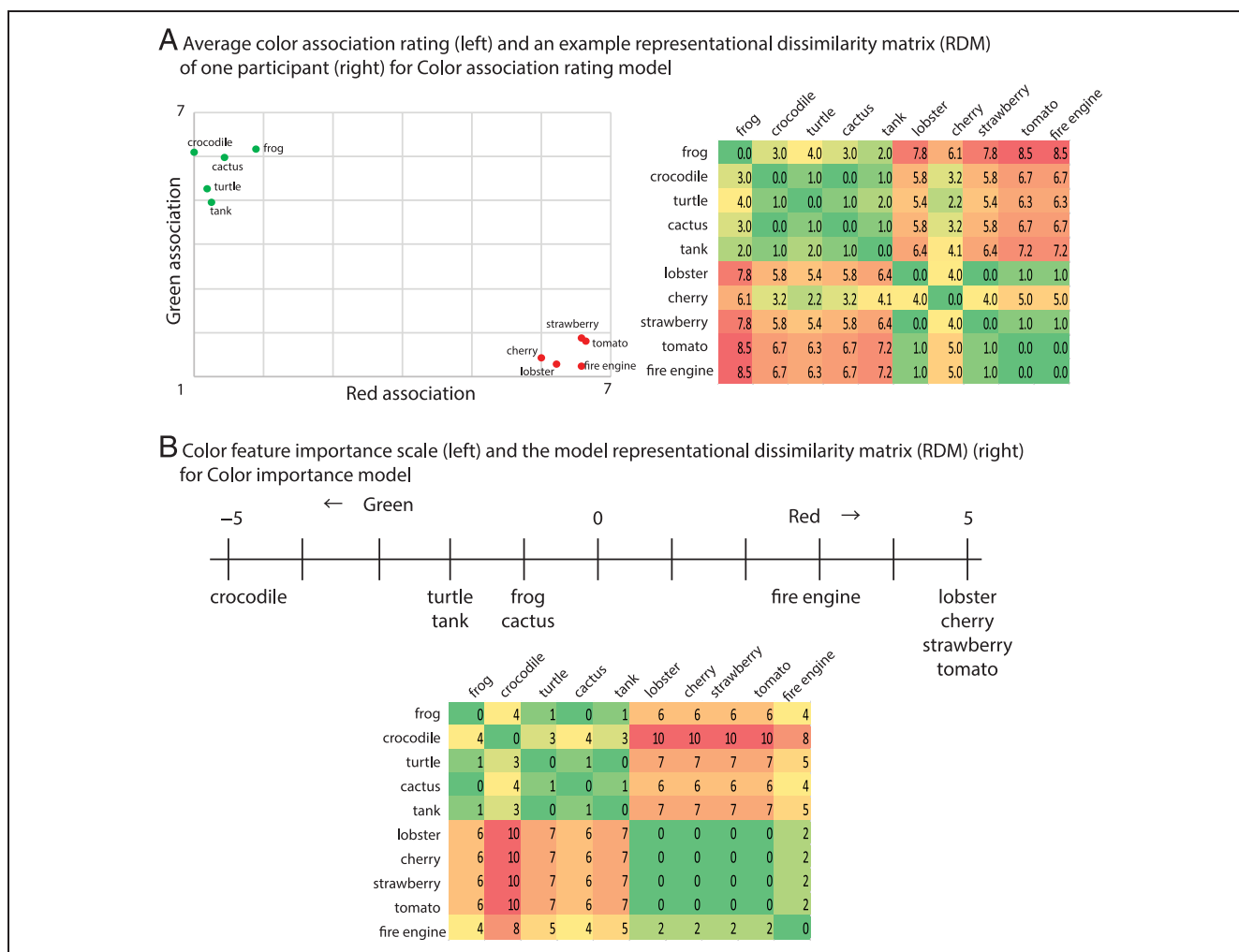


Figure 4. Color association ratings and color importance scale. (A) The graph on the left shows the average green-ness (y axis) and red-ness (x axis) scale rated for each object by the participants, and on the right, the graph shows an example model RDM of one participant by computing the Euclidean distance between each object pair. (B) The placement of the objects along the line for the color feature importance scale according to McRae and colleagues (2005). Distance between the points for each object pair was calculated and used for the color importance model RDM.

model RDM based on color importance scores (1 = color being less important feature, and 5 = color being very important feature of the object). The color importance scores were based on the ranking of the color feature in the semantic feature production norms by McRae and colleagues (McRae, Cree, Seidenberg, & McNorgan, 2005), except for “cactus” for which we used the association norms provided by Nelson, McEvoy, and Schreiber (2004). Because there were no listings for “fire engine” in neither of the databases, we substituted this value with that of “ambulance” in the McRae database. The color importance distance between the objects was calculated as the difference between the scores of each object, by placing green objects on one side of the axis and the red objects on the other side, and further away from the center as the color importance increased. Figure 4 (bottom) shows the color importance scores plotted in this way. Distances between each object pair served as the dissimilarity score for the model RDM of the color importance model.

For both models, the Spearman’s correlation between the model RDM and the neural data RDM was computed. Ten thousand permutations were performed to test for the significance of the fit. Computed r -maps for each participant for each task were then normalized to MNI space using the normalization parameter estimated during the segmentation of T1 image and smoothed with a 5-mm kernel FWHM.

At the group level, the normalized-smoothed r -maps for each participant were subjected to a second-level random effects analysis with nonsphericity correction for correlated repeated measures. This was carried out for each of the tasks for the two models. We applied the cluster defining voxel level threshold of $p < .001$ uncorrected, and then a cluster-level threshold of false discovery rate (FDR) $p < .05$ (Hayasaka & Nichols, 2003) was used to account for multiple comparisons. Furthermore, to see the extent of overlap between the tasks, we also ran a full-factorial design with the four levels (object naming and semantic judgment in Session 1, object naming and

Table 1. Overt Speech Performance during the Naming Tasks

<i>Task</i>	<i>Average (%)</i>	<i>Standard Deviation (%)</i>
Object naming (Session 1)	96	5
Object naming (Session 2)	96	6
Semantic judgment	99	2
Color naming*	100	1

* Although we expected typically green objects to be responded to as “green” and red object as “red,” some participants named other colors. As they were instructed to respond to what they think the typical color of the cued object is, there was no correct or incorrect response. Therefore, only no-response trials were scored as incorrect for the color naming task.

color naming in Session 2) as four factors of interest for both models. We searched for overlapping voxels that survived the above-mentioned threshold using the minimum statistic/conjunction null function of SPM12 (Nichols, Brett, Andersson, Wager, & Poline, 2005).

RESULTS

Behavioral Results

Overall, participants were highly accurate at overtly producing the words when prompted with a response cue (see Table 1 for the performance of each task). It is, thus, likely that the participants conformed to the task also

Table 2. Green–Red Mask

	<i>Regions</i>	<i>L/R</i>	<i>Cluster</i>	<i>Peak Coordinate</i>			<i>t Value</i>
			<i>Size</i>	<i>x</i>	<i>y</i>	<i>z</i>	
1	Thalamus	R	567	18	−18	8	5.52
	Thalamus	R		12	−12	18	2.62
	Caudate	R		18	8	22	2.22
2	Fusiform gyrus	R	1706	30	−6	−36	3.89
	Fusiform gyrus	R		40	−12	−40	3.31
	Fusiform gyrus	R		38	−24	−24	3.12
	Fusiform gyrus	R		40	−30	−22	3.08
	Middle temporal gyrus	R		56	−4	−25	3.00
	Middle temporal gyrus	R		62	0	−26	2.90
	Middle temporal gyrus	R		48	2	−32	2.63
	Inferior temporal gyrus	R		44	4	−42	3.45
	Inferior temporal gyrus	R		46	−36	−24	3.02
	Inferior temporal gyrus	R		58	−12	−34	2.63
	Inferior temporal gyrus	R		50	−14	−26	2.11
	Inferior temporal gyrus	R		46	−2	−34	1.99
	3	Inferior temporal gyrus		L	1629	−48	−52
Inferior temporal gyrus		L	−48	−46		−16	3.35
Inferior temporal gyrus		L	−42	−40		−28	2.51
Fusiform gyrus		L	−44	−40		−20	3.14
Fusiform gyrus		L	−28	−14		−36	2.83
Fusiform gyrus		L	−36	−28		−28	2.31
Middle occipital gyrus		L	−40	−60		0	2.73
Inferior occipital gyrus		L	−44	−70		−16	2.50
Inferior occipital gyrus		L	−46	−28		−22	2.39
Inferior occipital gyrus		L	−44	−30		−28	2.38
Parahippocampal gyrus		L	−30	−22		−22	2.13

Table 2. (continued)

	Regions	L/R	Cluster	Peak Coordinate			t Value		
			Size	x	y	z			
4	Supramarginal gyrus	L	614	-46	-38	28	3.29		
	Superior temporal gyrus	L		-50	-46	20	2.84		
	Superior temporal gyrus	L		-54	-34	20	2.78		
5	Calcarine gyrus	L	2386	-4	-66	12	3.04		
	Calcarine gyrus	R		16	-86	8	2.77		
	Calcarine gyrus	R		10	-85	6	2.68		
	Fusiform gyrus	R		38	-54	-10	2.89		
	Fusiform gyrus	R		30	-58	-10	2.69		
	Fusiform gyrus	R		28	-62	-14	2.62		
	Lingual	R		22	-64	-10	2.83		
	Superior occipital gyrus	L		-18	-70	32	2.78		
	Middle occipital gyrus	L		-22	-62	34	2.75		
	Precuneus	L		-18	-64	32	2.69		
	Cuneus	L		-14	-60	24	2.55		
	6	Putamen		L	107	-22	4	10	3.09
	7	Precuneus		R	269	26	-54	24	2.15
Inferior parietal gyrus		R	40	-54		38	1.79		
8	Superior frontal gyrus (orbitalis)	L	1037	-14	20	-18	2.96		
	Inferior frontal gyrus (triangularis)	L		-34	26	14	2.70		
	Inferior frontal gyrus (triangular)	L		-42	28	4	2.62		
	Inferior frontal gyrus (triangular)	L		-44	22	14	2.59		
	Inferior frontal gyrus (triangular)	L		-58	28	20	2.17		
	Inferior frontal gyrus (triangular)	L		-54	28	2	1.99		
	Caudate nucleus	L		-12	10	4	2.62		
	Superior frontal gyrus (orbitalis)	L		-16	42	-20	2.53		
	Putamen	L		-20	18	8	2.36		
9	Cerebellum	L	139	-24	-38	-52	2.61		
	Superior frontal gyrus (medial)	R		157	2	40	30	2.49	
10	Anterior cingulate cortex	R	157	12	46	20	2.09		
	Anterior cingulate cortex	R		4	44	20	1.96		
	Middle frontal gyrus	L		110	-24	24	34	2.28	
12	Supplementary motor area	R	125	12	-20	60	2.37		
	Superior frontal gyrus	R		22	-4	70	2.36		
	Superior frontal gyrus	R		20	-10	64	2.04		
13	Caudate nucleus	R	143	12	24	2	2.33		
	Caudate nucleus	R		20	26	4	2.10		
	Putamen	R		28	14	-4	2.23		
14	Precuneus	R	104	8	-70	32	2.24		
	Precuneus	R		14	-60	32	2.09		

L = left; R = right.

during the covert speech-only trials so we included all word trials for the imaging analyses.

The correlation between the individual color association rating model RDM and the color feature importance model was very high (average $R = .827$, min = 0.606, max = 0.896). This was expected given that all objects were HCD objects. We tested RSA on both models, however, given the individual differences in the degree to which the two models correlated.

Decoding Classifier

Circle Task

During the circle task, participants were presented with either a red or a green circle moving either inward or outward, and they were instructed to indicate via button press whether the motion was in the same or in the opposite direction from the previous trial (1-back task). Using the searchlight approach, we searched for voxels that could decode green from red above chance level. At a lenient threshold of $p < .05$ voxel-level uncorrected, we observed several clusters in both hemispheres, including the bilateral calcarine, lingual, and fusiform gyri, extending to the precuneus (Figure 3). Clusters

were not limited to visual areas but were found also in the bilateral frontal gyri, and the bilateral inferior temporal lobe, among other areas (see Table 2 for a full report). These clusters were used as a mask for the RSA analyses.

RSAs

Whole-brain Analysis

As expected, at the whole-brain level, a wide range of areas showed high correlation with both of the model RDMs for the color naming task (Figure 5, Tables 3 and 4). The object naming task also showed areas that could dissociate between green and red objects. The semantic judgment task also showed areas that dissociated green from red. Both models showed fewer areas to be significant for this semantic judgment task compared with the other two tasks.

Using conjunction analysis across the different tasks, we identified areas showing overlap between the tasks (see Figure 6, top and middle rows). For the color importance model, clusters in the bilateral fusiform gyri overlapped across all three tasks. For the color association rating model, a cluster in the right posterior middle temporal

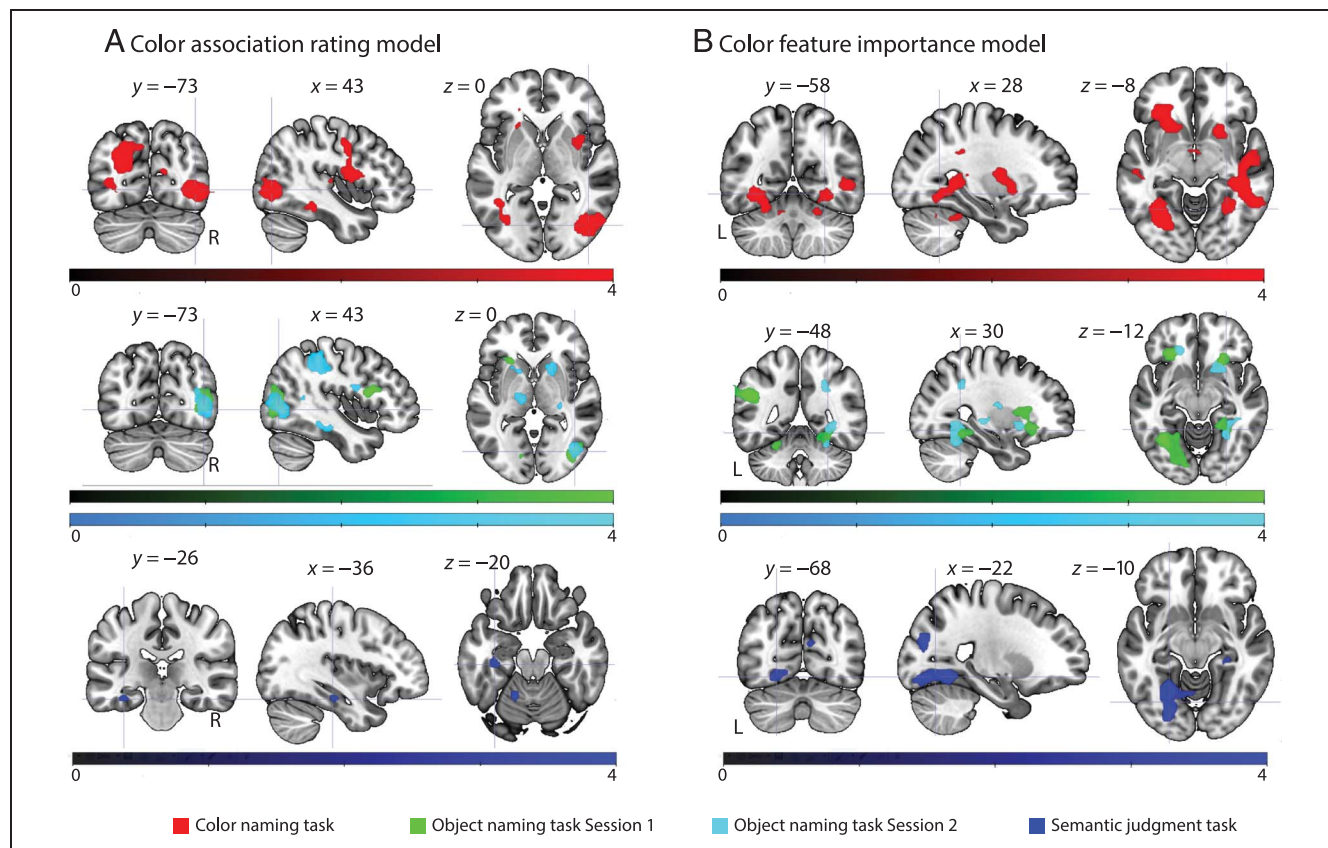


Figure 5. Correlations between the brain RDM and the two model RDMs in the whole-brain analysis. Significant clusters that showed a high correlation between the model and the brain RDMs (thresholded at cluster level $pFDR < 0.05$, cluster defining voxel level $p < .001$, uncorrected) are overlaid on the MNI template brain. Upper row: color naming task; middle row: object naming task (green = Session 1, light blue = Session 2); bottom row: semantic judgment task. Color bars represent the t values of the voxels. Note, because of thresholding at the cluster-size statistics, not all voxels ($p < .001$ uncorrected) are shown on the figure.

Table 3. Color Individual Association Model

		<i>L/R</i>	<i>p(FDR)</i>	<i>Size</i>	<i>Cluster-peak Voxel</i>			<i>t Value</i>
					<i>x</i>	<i>y</i>	<i>z</i>	
<i>Color Naming Task</i>								
1	Inferior occipital gyrus	R	0	417	41	-72	-3	6.42
2	Superior occipital gyrus	L	0	919	-25	-72	33	6.39
	Precuneus	L			-7	-70	43	4.45
3	Putamen	R	0	856	26	-5	13	6.35
	Rolandic operculum	R			51	-2	18	4.72
	Precentral gyrus	R			43	-2	40	4.47
4	Middle cingulate cortex	R	0	370	18	-37	30	6.17
5	Precentral gyrus	L	0	120	-50	-2	20	5.15
6	Inferior frontal gyrus (orbitalis)	L	0	224	-22	33	-10	5.09
	Insula	L			-22	23	5	3.72
7	Middle cingulate cortex	L	0		-10	-25	40	4.08
8	Fusiform gyrus	L	0	330	-40	-55	-5	4.8
	Middle occipital gyrus	L			-37	-72	8	3.97
9	Inferior frontal gyrus (triangularis)	L	0	61	-32	16	20	4.64
10	Cerebellum	L	0	91	-12	-62	-25	4.52
11	Cerebellum	R	0	111	23	-60	-25	4.22
12	Superior frontal gyrus	L	0	117	-17	18	43	4.15
	Anterior cingulate cortex	L			-10	16	30	3.63
13	Fusiform gyrus	R	0.001	30	43	-35	-15	4.1
14	Middle cingulate cortex	R	0	72	16	16	33	4.05
	Anterior cingulate cortex	R			18	26	23	3.84
15	Insula	L	0.002	24	-27	-7	20	4.03
	Caudate nucleus	L			-22	-2	28	3.74
16	Supplementary motor area	L	0	54	-10	-15	60	4.01
17	Rectus gyrus	L	0.002	24	-12	16	-13	3.83
	Olfactory gyrus	L			-7	8	-20	3.56
18	Calcarine gyrus	R	0.002	24	13	-72	18	3.83
19	Superior temporal gyrus	R	0.001	28	51	-10	-10	3.71
20	Postcentral gyrus	L	0.045	10	-47	-7	38	3.65
<i>Object naming task Session 1</i>								
1	Inferior occipital gyrus	R	0	281	41	-80	-3	4.67
	Middle occipital gyrus	R			43	-72	13	4.53
2	Putamen	L	0.001	89	-27	-7	15	4.6
3	Supramarginal gyrus	L	0.003	64	-45	-30	33	4.56
4	Inferior frontal gyrus (opercularis)	R	0	107	43	11	15	4.31

Table 3. (continued)

		<i>L/R</i>	<i>p(FDR)</i>	<i>Size</i>	<i>Cluster-peak Voxel</i>			<i>t Value</i>
					<i>x</i>	<i>y</i>	<i>z</i>	
5	Superior frontal gyrus	L	0.001	81	-17	11	43	4.23
	Supplementary motor area	L			-15	-12	50	3.76
6	Insula	L	0.001	78	-25	23	-3	4.18
7	Anterior cingulate cortex	R	0.013	42	11	31	-8	4.16
8	Lingual gyrus	L	0.013	43	-12	-80	-8	4.09
<i>Object naming task Session 2</i>								
1	Middle temporal gyrus	R	0	270	43	-70	0	5.66
	Middle occipital gyrus	R			43	-77	8	4.82
2	Inferior parietal gyrus	R	0	981	36	-40	48	5.45
	Precuneus	R			3	-55	43	4.45
	Postcentral	R			21	-37	50	4.33
3	Inferior frontal gyrus (opercularis)	L	0	695	-27	1	25	5.25
	Middle frontal gyrus	L			-27	3	45	4.76
	Middle cingulate gyrus	L			-17	-25	50	4.75
4	Caudate nucleus	R	0	275	13	13	-8	4.99
	Putamen	R			26	18	-10	4.16
5	Caudate nucleus	L	0	252	-12	13	-5	4.86
	Inferior frontal gyrus (orbitalis)	L			-20	36	-10	4.7
6	Inferior temporal gyrus	L	0	188	-45	-17	-20	4.84
	Hippocampus	L			-25	-12	-23	4.16
	Middle temporal gyrus	L			-55	-12	-18	3.96
7	Supplementary motor area	R	0	138	21	-5	45	4.7
	Superior frontal gyrus	R			18	6	48	4.64
	Middle cingulate gyrus	R			21	-2	35	3.77
8	Postcentral gyrus	L	0	108	-40	-27	38	4.59
9	Cerebellum	R	0.002	23	21	-50	-38	4.33
10	Cerebellum	R	0	40	18	-55	-23	4.13
11	Inferior temporal gyrus	L	0.004	20	-40	1	-33	4.11
12	Hippocampus	R	0	80	28	-25	0	4.11
	Insula	R			31	-22	13	4.05
	Thalamus	R			21	-17	13	3.56
13	Inferior frontal gyrus (opercularis)	R	0	33	36	13	33	4.05
14	Cerebellum	L	0.003	21	-20	-55	-33	3.99
15	Fusiform gyrus	R	0	40	43	-27	-18	3.98
16	Rolandic operculum	R	0.002	23	41	-2	20	3.73
17	Putamen	R	0.048	9	33	-7	10	3.57

Table 3. (continued)

		L/R	<i>p</i> (FDR)	Size	Cluster-peak Voxel			<i>t</i> Value
					<i>x</i>	<i>y</i>	<i>z</i>	
<i>Semantic judgment task</i>								
1	Superior frontal gyrus	L	0.038	28	−25	−2	45	4.49
2	Cerebellum	R	0	166	41	−60	−38	4.33
3	Putamen	L	0.013	46	−22	13	−3	4.31
4	Inferior temporal gyrus	L	0.006	61	−45	−12	−25	4.13
	Fusiform gyrus	L			−37	−25	−20	3.82
5	Cerebellum	L	0.002	81	−17	−55	−23	4.11
6	Putamen	R	0.029	32	23	3	−8	4.04
7	Caudate nucleus	R	0.045	25	11	26	8	3.98
8	Parahippocampal gyrus	R	0.013	43	31	−2	−33	3.95
9	Parahippocampal gyrus	R	0.013	44	21	−37	−5	3.81

L = left; R = right.

gyrus showed overlap. Because of different statistics applied, some areas showed significant clusters that were not always significant on the whole-brain level when each task was analyzed separately.

Within the Circle Task Mask

Because the chosen green and red objects were not fully balanced in terms of other factors than color, differentiating patterns for the two object groups may reflect processing that could be attributed to other factors (e.g., edible objects for the red objects, and animals for the green objects). To exclude factors other than color-related processing, we limited our search area to the green–red mask

obtained from the circle task, as visual input in the circle task was only green or red colored circles.

Color Association Rating Model

Within the green–red mask, the color naming task showed clusters in the right fusiform, left precuneus, left inferior temporal gyrus, and left cuneus. For Session 2 of the object naming task, a cluster in the bilateral precuneus and a cluster in the right fusiform gyrus were found to be significant. No significant clusters within the mask were observed for Session 1 of the object naming task and for the semantic judgment task. No clusters survived significance for the conjunction analysis across the three tasks.

Table 4. Color Feature Importance Model

		L/R	<i>p</i> (FDR)	Cluster-peak Voxel			<i>t</i> Value
				<i>x</i>	<i>y</i>	<i>z</i>	
<i>Color Naming Task</i>							
1	Fusiform gyrus	L	0	−30	−65	−5	6.3
	Cerebellum	L		−25	−57	−18	4.06
	Cerebellum	L		−12	−65	−28	3.8
2	Middle/posterior cingulate cortex	R	0	18	−37	33	5.57
	Hippocampus	R		41	−35	−8	5.3
	Inferior frontal gyrus (opercularis)	R		53	8	8	5.22
3	Anterior cingulate	L	0	−12	18	28	5.17
	Middle frontal gyrus	L		−35	33	15	4.99
	Insula	L		−22	21	5	4.84

Table 4. (continued)

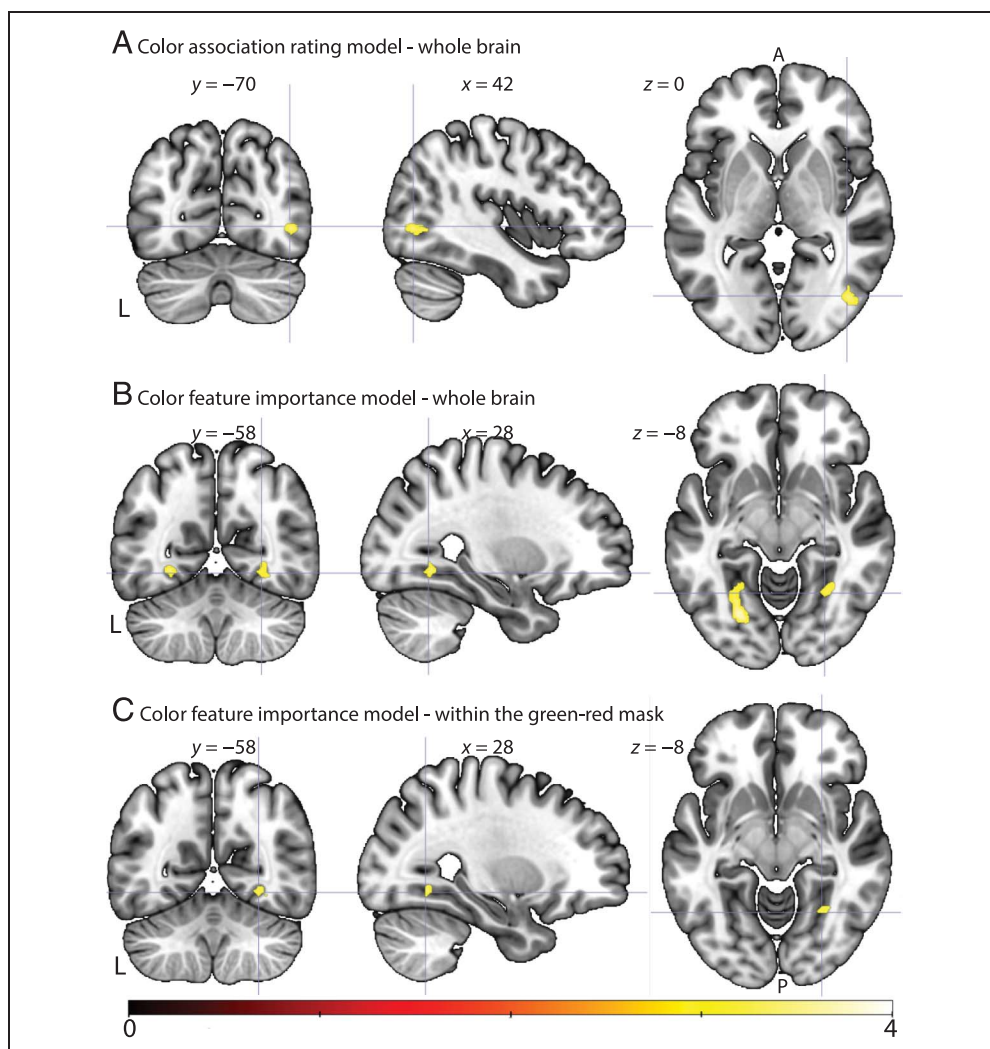
		L/R	<i>p</i> (FDR)	Cluster-peak Voxel			<i>t</i> Value
				<i>x</i>	<i>y</i>	<i>z</i>	
4	Supramarginal gyrus	L	0	-47	-45	33	4.73
5	Postcentral gyrus	L	0	-25	-35	45	4.7
	Supplementary motor area	L		-10	-17	55	4.02
	Middle cingulate	L		-17	-27	53	3.88
6	Inferior temporal gyrus	L	0	-42	-22	-15	4.69
7	Superior anterior cingulate cortex	R	0	18	23	25	4.61
	Middle cingulate	R		18	18	33	4.44
8	Cerebellum	R	0	23	-40	-28	4.58
9	Cerebellum	L	0	-5	-30	-35	4.57
10	Superior occipital gyrus	L	0	-22	-75	28	4.46
	Middle occipital gyrus	L		-22	-80	20	4.43
11	Thalamus	R	0	11	-12	5	4.16
12	Thalamus	L	0	-15	-22	5	3.97
13	Superior frontal gyrus (medial)	L	0.034	-10	43	35	3.89
14	Middle temporal gyrus	L	0.034	-42	-50	8	3.76
15	Precentral gyrus	R	0.011	53	1	48	3.72
16	Cerebellum	L	0.034	-5	-5	-5	3.66
17	Middle temporal gyrus	L	0.042	-55	-50	5	3.64
18	Medial superior frontal gyrus	L	0.026	-10	-80	-28	3.58
<i>Object naming task Session 1</i>							
1	Supramarginal gyrus	L	0	-55	-35	28	6.02
	Postcentral gyrus	L		-50	-25	28	5.75
	Precentral gyrus	L		-55	6	15	5.35
2	Fusiform gyrus	L	0	-32	-62	-5	5.43
	Lingual gyrus	L		-27	-72	-5	4.42
3	Middle cingulate	L	0	-12	3	40	5.07
4	Inferior frontal gyrus (opercularis)	R	0	43	18	13	5.06
	Insula	R		26	23	-10	4.58
5	Inferior frontal gyrus (triangularis)	L	0	-32	38	10	4.91
6	Fusiform gyrus	R	0	21	-42	-15	4.47
7	Middle occipital gyrus	R	0	41	-80	0	4.22
8	Superior temporal gyrus	R	0	71	-42	23	4.19
9	Supplementary motor area	R	0.004	13	-20	60	4.15
10	Superior temporal gyrus	R	0	66	-17	5	4.14
11	Insula	L	0	-30	-30	28	4.07
12	Supplementary motor area	R	0	13	-5	55	3.97
13	Middle temporal gyrus	L	0	-52	-22	-5	3.92

Table 4. (continued)

		L/R	<i>p</i> (FDR)	Cluster-peak Voxel			<i>t</i> Value
				<i>x</i>	<i>y</i>	<i>z</i>	
14	Superior temporal gyrus	L	0.004	-67	-42	15	3.77
15	Middle temporal gyrus	L	0.02	-55	-12	-18	3.74
16	Precentral gyrus	R	0.005	38	-10	45	3.71
17	Fusiform gyrus	R	0.041	33	-5	-35	3.67
18	Supplementary motor area	L	0.02	-10	-17	60	3.66
<i>Object naming task Session 2</i>							
1	Putamen	R	0	18	11	-5	4.89
2	Lingual gyrus	R	0	28	-52	-5	4.74
	Parahippocampal gyrus	R		31	-42	-8	4.12
	Cerebellum	R		21	-55	-25	4.11
3	Precentral	L	0	-25	-15	45	4.62
	Paracentral	L		-12	-25	55	4.54
	Inferior parietal gyrus	L		-35	-30	38	4.02
4	Angular gyrus	R	0	26	-47	35	4.59
5	Putamen	L	0	-22	16	3	4.42
6	Postcentral	R	0.024	26	-30	45	4.12
7	Inferior frontal gyrus (orbitalis)	L	0	-20	33	-10	4.06
8	Inferior temporal gyrus	R	0.024	46	-25	-20	3.99
9	Hippocampus	R	0.002	31	-25	-3	3.96
	Thalamus	R		26	-20	3	3.68
10	Thalamus	L	0.024	-17	-10	0	3.89
11	Putamen	R	0.002	26	-12	15	3.75
	Insula	R		36	-5	18	3.57
12	Lingual gyrus	L	0.028	-17	-77	-5	3.55
<i>Semantic judgment task</i>							
1	Lingual gyrus	L	0	-25	-57	-10	4.86
2	Superior occipital gyrus	L	0	-22	-80	23	4.74
3	Posterior cingulate cortex	R	0	16	-37	23	4.43
	Middle cingulate cortex	R		8	-27	23	4.1
	Precuneus	R		16	-50	28	3.94
4	Supplementary motor area	L	0.002	-10	-20	50	4.09
5	Hippocampus	L	0.002	-30	-27	-15	3.92
6	Parahippocampal gyrus	R	0.002	28	-32	-10	3.75
7	Middle temporal gyrus	L	0.047	-50	-10	-20	3.67
8	Postcentral gyrus	L	0.047	-17	-42	60	3.66

L = left; R = right.

Figure 6. Overlapping areas across the three tasks. (A) For the color association rating model, a right posterior middle temporal cluster showed an overlap across the three tasks (thresholded at cluster defining voxel level $p < 0.001$, uncorrected, cluster level $P_{FDR} < 0.05$) in the whole brain analysis. (B) For the Color feature importance model, overlapping clusters were found in the bilateral fusiform gyri in the whole brain analysis. (C) Within the Green-red mask (small volume corrected), the right fusiform gyrus was observed. All clusters are thresholded at cluster defining voxel level $p < 0.001$, uncorrected, cluster level $P_{FDR} < 0.05$. Color-bar shows the t-value of the voxels).



Color Feature Importance Model

The color naming task revealed significant clusters in the bilateral fusiform gyri. Whereas several clusters in the left hemisphere were significant for Session 1 of the object naming task, only the right lingual and fusiform gyri clusters were significant for Session 2 of the object naming task. For the semantic judgment task, a cluster in the left lingual gyrus was found to be significant. The conjunction analysis for the three tasks revealed significant clusters in the right posterior fusiform gyrus (Figure 6, bottom row).

DISCUSSION

In this study, we investigated the retrieval of conceptual color knowledge in different tasks, all of which involved the presentation of typically green or red objects (e.g., cactus, tomato) as black line drawings. As color information was not provided in the input, we considered color-specific hemodynamic brain activations as evidence for the retrieval of conceptual color knowledge about the objects presented. In one task, participants were asked

to name the color of the depicted object. In a second task, they were asked to name the object itself, and in a third task, they were asked to perform a semantic judgment on the object (respond covertly/overtly whether the object was natural or man-made).

We reasoned that naming the color of an object would necessarily involve the retrieval of conceptual color knowledge and hence activate brain regions differentially responding to green or red objects. To the degree that color information would also be retrieved in the other two tasks, the activation patterns observed in these tasks would overlap with the pattern observed in the color naming task. If there was no overlap, hence no evidence for the retrieval of color information in the object naming and semantic judgement tasks, one could conclude that the retrieval of color knowledge hinges on its necessity for the task at hand. If, on the other hand, there was evidence for the retrieval of color information in all three tasks, one could conclude that (at least important, such as “color” for HCD objects) attributes are automatically co-activated with their object concepts, irrespective of whether the attribute information is relevant for a given task. We were

particularly interested in a third option, namely, that there would be evidence for the retrieval of color information in color and object naming but not in the semantic judgment task. Such a result pattern would suggest that the retrieval of the color attribute might assist the word production in picture naming.

To identify brain activation patterns related to the green color and red color processing, we used the RSA method (Nili et al., 2014; Kriegeskorte et al., 2008; Kriegeskorte, Goebel, & Bandettini, 2006) as this allows us to build a model that is not binary. We compared the RDM of the hemodynamic brain activation (brain RDM) to two models. The first model, a color association rating model, graded the green-ness and red-ness levels of the objects according to the strength of the individual color associations of our participants. The second model, the color feature importance model, assigned high green or red values to an object if the color was an important feature for that object in a semantic feature database (McRae et al., 2005). The use of these models was motivated by behavioral evidence that the association strength between an object name and its color modulates the strength of the color Stroop effect (Scheibe et al., 1967) and hence presumably the degree of activation of the color concept or the color name.

As typically green and red objects unavoidably also differ in other respects (e.g., shape, natural life size), we not only conducted conjunction analyses of overlapping color-sensitive brain regions across the whole brain but also in a restricted search space defined by an additional functional color perception localizer task (see Hsu, Frankland, & Thompson-Schill, 2012; Hsu, Kraemer, Oliver, Schlichting, & Thompson-Schill, 2011; Simmons et al., 2007; Beauchamp, Haxby, Jennings, & DeYoe, 1999; Chao & Martin, 1999; Zeki & Marini, 1998, for a similar approach). Because this task only used color but no object-specific features, we reasoned that using it as a mask would filter out hemodynamic brain responses to possible confounding noncolor differences between green and red objects.

In the whole-brain search analysis, activation in the bilateral fusiform gyri, an area that is known to be sensitive to perceived color (Human V4; Zeki, 1993, p. 137; Zeki et al., 1991), correlated with the color importance model in all three tasks, suggesting that color knowledge about HCD objects was retrieved irrespective of whether a task required accessing the object color or not. Crucially, this result also suggests that color knowledge was not necessarily retrieved for the purpose of naming the object. Instead, when presented with an achromatic picture of an HCD object, information about color seems to be accessed anyway, and the more so, the more important color is for the object at hand. Consequently, with respect to our research question about the amount of conceptual information that is used to activate the lemma of a to-be-named object, our results suggest that at least one type of nonminimal conceptual information, color, would be

available to be used for lexical access when the object is HCD. Our data, however, do not allow the conclusion that it is retrieved for that purpose or even that it is actually used for object naming.

Our results confirm previous findings suggesting that the retrieval of conceptual color knowledge about HCD objects involves the fusiform gyri (Bannert & Bartels, 2013, 2018; Fernandino et al., 2016; Hsu et al., 2011; Simmons et al., 2007). Most of these studies elicited the retrieval of conceptual color knowledge by presenting their participants with words denoting HCD objects and asking them to perform various tasks requiring use of the color information (Fernandino et al., 2016; Hsu et al., 2011; Simmons et al., 2007). Analogous to our use of a color importance model, Fernandino and colleagues (2016) investigated the contribution of sensory-motor properties to the neural representations of concepts by taking the relative importance of properties for different concepts into account from an embodied cognition perspective. During fMRI scanning, they presented their participants with a large number of words that had been rated with respect to the relevance of different properties (color, shape, sound, visual motion, and manipulation) for their meaning. Using a multivariate regression analysis of the fMRI data, the authors identified brain regions that were sensitive to the relevance of the different properties. For color, they found (among other regions) a lingual/fusiform region corresponding almost exactly to our region of overlap in the left hemisphere. We concur with the authors' conclusion that "the retrieval of concepts associated with salient colour attributes involves the activation of perceptually encoded colour information."

Compared with the rather robust neuroimaging evidence that words denoting HCD objects elicit activation of the fusiform gyri, it was, to date, not so clear, whether the same holds true for the naming of achromatic picture stimuli of such objects. Bannert and Bartels (2013) presented their participants with achromatic pictures of HCD objects and asked them to perform a task that did not require accessing the object color (rotation judgment). They trained a linear classifier to decode the object color from the participants' hemodynamic brain activation data and found that it could be predicted above chance from primary visual cortex as well as from V4 activation patterns. This study suggests that not only words but also viewing HCD objects even in grayscale format elicits color information. Our result suggests that this also holds for production of the name of the object.

Most similar to our study, Chao and Martin (1999) asked their participants to name achromatic HCD objects or to name their color during PET scanning. Compared with a baseline task of passively viewing grayscale Mondrians, both naming the color and naming the objects activated the fusiform gyri bilaterally, whereas this activation was not observed when directly comparing color and object naming. The authors interpret the activation of the fusiform gyri during the naming of achromatic objects as

evidence for an involvement of this region in “object identification, but not colour perception.” Note, however, that their result pattern is entirely consistent with our assumption that color knowledge is not only retrieved when naming the color of achromatic HCD objects but also when naming the object itself. Insofar as the fusiform gyri are involved in color knowledge retrieval, a direct comparison of the two tasks would be expected to show no differential activation in this region. Whereas the univariate analysis of the blood flow changes measured with PET in their study could not tell whether fusiform activation during object naming was because of object identification or color processing, the RSA used in our study showed that the fusiform gyri were indeed sensitive to the red–green distinction and, hence, involved in color processing, in both color and object naming tasks.

In summary, our study confirmed the finding of previous studies that the retrieval of color knowledge about HCD objects activates a brain region involved in the perceptual processing of color. Furthermore, our results suggest that color knowledge is not only retrieved based on the names of objects with a typical color but also upon viewing achromatic depictions of those objects. In the latter case, color knowledge may be retrieved based on the recognition of the objects and then potentially used to access the object names. As it has been shown that depicted objects are tacitly named even when no overt naming is required (Meyer & Damian, 2007), it is also possible that the retrieval of color knowledge followed the retrieval of the object names in all our tasks.

Like most other studies on the retrieval of conceptual color knowledge, we used in addition a perceptual color processing localizer task. This task served to distinguish between color-specific neural activation and activation because of potential noncolor differences between HCD objects of different colors. In our study, only the activation pattern of the right but not the left fusiform gyrus was included in the activation pattern of the localizer task. We can conclude that activation of the right fusiform gyrus reliably reflected processing of the object color, whereas activation of the left fusiform gyrus could have been because of other object properties than color. Note, however, that the perceptual color localizer task that we used might not have been suitable for capturing the retrieval process related to the conceptual color knowledge. We think that the latter explanation is more likely for two reasons. First, there are studies that used word stimuli and reported left fusiform activation for conceptual color processing (Bannert & Bartels, 2018; Hsu et al., 2011; Simmons et al., 2007). Thus, the activation in the left fusiform region is more likely to have been caused by color processing, rather than reflecting a non-color-related processing that might have systematically been present for the green and the red objects that we tested. Second, in our study, the region showing overlap across the three tasks was about 15 mm more anterior ($y = -57$) in the left hemisphere than in the right hemisphere ($y =$

-72). In a review article on the human color-sensitive cortex, Bartels and Zeki (2000) argue for a subdivision into a more posterior perceptual area ($V4$) and a more anterior area ($V4\alpha$) that is sensitive to whether objects are normally or abnormally colored. In other words, this more anterior area may be influenced by conceptual color knowledge processing rather than reflecting a process related to perceptual color.

The color-specific activation of the fusiform gyri corresponded to a theoretical model that represented the relative importance of color for the different objects, but not to a model that represented how strongly the colors red or green were associated with them. We think that this result may be because of the fact that the individual color association model was based on the participants’ ratings of how strongly they associated red or green with the different objects but did not take into account that individual participants might rather associate a different color with an object and hence might not necessarily reflect the color evoked when participants saw the depicted achromatic objects.

Conclusions

When seeing objects that have typical colors (HCD objects), activation of our color-sensitive cortex reflects their typical color even if it is not present in the visual input and not relevant for the task at hand. The color-sensitive cortex thus must be activated by conceptual color representations, our stored knowledge about the color of the objects, in a top–down manner, or even be part of the conceptual color representations as assumed by embodied cognition theories. The degree of activation depends on how important a property color is for an object, suggesting that the importance of a property for an object is somehow reflected in its conceptual representation.

Acknowledgments

We would like to thank Giacomo Tartaro for assisting in data collection and Heike Uden for creating the stimulus pictures. We also thank Matthias Ekman and David Richter for help with the decoding classifier analyses.

Corresponding author: Atsuko Takashima, Radboud University Donders Centre for Cognitive Neuroimaging, Nijmegen 6500 HE, The Netherlands, or via e-mail: atsuko.takashima@donders.ru.nl.

Data Availability Statement

Materials and data for the study are available at [di.dccn.DSC_3021005.23_080](https://doi.org/10.1177/124219081410000002068).

Author Contributions

Atsuko Takashima: Data curation; Formal analysis; Investigation; Methodology; Visualization; Writing—Original draft; Writing—Review & editing. Francesca Carota:

Formal analysis; Investigation; Methodology; Writing—Original draft; Writing—Review & editing. Vincent Schoots: Conceptualization; Data curation; Investigation; Methodology; Writing—Original draft; Writing—Review & editing. Alexandra Redmann: Conceptualization; Methodology; Writing—Original draft; Writing—Review & editing. Janneke Jehee: Conceptualization; Formal analysis; Writing—Original draft; Writing—Review & editing. Peter Indefrey: Conceptualization; Funding acquisition; Project administration; Resources; Supervision; Writing—Original draft; Writing—Review & editing.

Funding Information

This study was supported by the Deutsche Forschungsgemeinschaft (DFG; <https://dx.doi.org/10.13039/501100001659>), grant number: Sonderforschungsbereich (SFB) 991; and Max Planck Institute for Psycholinguistics.

Diversity in Citation Practices

Retrospective analysis of the citations in every article published in this journal from 2010 to 2021 reveals a persistent pattern of gender imbalance: Although the proportions of authorship teams (categorized by estimated gender identification of first author/last author) publishing in the *Journal of Cognitive Neuroscience (JoCN)* during this period were $M(\text{an})/M = .407$, $W(\text{oman})/M = .32$, $M/W = .115$, and $W/W = .159$, the comparable proportions for the articles that these authorship teams cited were $M/M = .617$, $W/M = .250$, $M/W = .067$, and $W/W = .067$ (Postle and Fulvio, *JoCN*, 34:1, pp. 1–3). Consequently, *JoCN* encourages all authors to consider gender balance explicitly when selecting which articles to cite and gives them the opportunity to report their article's gender citation balance.

REFERENCES

- Abdel Rahman, R., & Sommer, W. (2003). Does phonological encoding in speech production always follow the retrieval of semantic knowledge?: Electrophysiological evidence for parallel processing. *Cognitive Brain Research*, 16, 372–382. [https://doi.org/10.1016/S0926-6410\(02\)00305-1](https://doi.org/10.1016/S0926-6410(02)00305-1), PubMed: 12706217
- Bannert, M. M., & Bartels, A. (2013). Decoding the yellow of a gray banana. *Current Biology*, 23, 2268–2272. <https://doi.org/10.1016/j.cub.2013.09.016>, PubMed: 24184103
- Bannert, M. M., & Bartels, A. (2018). Human V4 activity patterns predict behavioral performance in imagery of object color. *Journal of Neuroscience*, 38, 3657–3668. <https://doi.org/10.1523/jneurosci.2307-17.2018>, PubMed: 29519852
- Bartels, A., & Zeki, S. (2000). The architecture of the colour centre in the human visual brain: New results and a review. *European Journal of Neuroscience*, 12, 172–193. <https://doi.org/10.1046/j.1460-9568.2000.00905.x>, PubMed: 10651872
- Beauchamp, M. S., Haxby, J. V., Jennings, J. E., & DeYoe, E. A. (1999). An fMRI version of the Farnsworth–Munsell 100-hue test reveals multiple color-selective areas in human ventral occipitotemporal cortex. *Cerebral Cortex*, 9, 257–263. <https://doi.org/10.1093/cercor/9.3.257>, PubMed: 10355906
- Bierwisch, M., & Schreuder, R. (1992). From concepts to lexical items. *Cognition*, 42, 23–60. [https://doi.org/10.1016/0010-0277\(92\)90039-K](https://doi.org/10.1016/0010-0277(92)90039-K), PubMed: 1582158
- Bird, C. M., Berens, S. C., Horner, A. J., & Franklin, A. (2014). Categorical encoding of color in the brain. *Proceedings of the National Academy of Sciences, U.S.A.*, 111, 4590–4595. <https://doi.org/10.1073/pnas.1315275111>, PubMed: 24591602
- Bramão, I., Faisca, L., Forkstam, C., Reis, A., & Petersson, K. M. (2010). Cortical brain regions associated with color processing: An fMRI study. *Open Neuroimaging Journal*, 4, 164–173. <https://doi.org/10.2174/1874440001004010164>, PubMed: 21270939
- Bramão, I., Reis, A., Petersson, K. M., & Faisca, L. (2011). The role of color information on object recognition: A review and meta-analysis. *Acta Psychologica*, 138, 244–253. <https://doi.org/10.1016/j.actpsy.2011.06.010>, PubMed: 21803315
- Brooks, J. L. (2012). Counterbalancing for serial order carryover effects in experimental condition orders. *Psychological Methods*, 17, 600–614. <https://doi.org/10.1037/a0029310>, PubMed: 22799624
- Brouwer, G. J., & Heeger, D. J. (2009). Decoding and reconstructing color from responses in human visual cortex. *Journal of Neuroscience*, 29, 13992–14003. <https://doi.org/10.1523/JNEUROSCI.3577-09.2009>, PubMed: 19890009
- Brouwer, G. J., & Heeger, D. J. (2013). Categorical clustering of the neural representation of color. *Journal of Neuroscience*, 33, 15454–15465. <https://doi.org/10.1523/JNEUROSCI.2472-13.2013>, PubMed: 24068814
- Carota, F., Nili, H., Pulvermüller, F., & Kriegeskorte, N. (2021). Distinct fronto-temporal substrates of distributional and taxonomic similarity among words: Evidence from RSA of BOLD signals. *Neuroimage*, 224, 117408. <https://doi.org/10.1016/j.neuroimage.2020.117408>, PubMed: 33049407
- Chao, L. L., & Martin, A. (1999). Cortical regions associated with perceiving, naming, and knowing about colors. *Journal of Cognitive Neuroscience*, 11, 25–35. <https://doi.org/10.1162/089892999563229>, PubMed: 9950712
- Collins, A. M., & Loftus, E. F. (1975). A spreading-activation theory of semantic processing. *Psychological Review*, 82, 407–428. <https://doi.org/10.1037/0033-295X.82.6.407>
- Dalrymple-Alford, E. C., & Azkoul, J. (1972). The locus of interference in the Stroop and related tasks. *Perception & Psychophysics*, 11, 385–388. <https://doi.org/10.3758/BF03206273>
- Faul, F., Erdfelder, E., Lang, A.-G., & Buchner, A. (2007). G*power 3: A flexible statistical power analysis program for the social, behavioral, and biomedical sciences. *Behavior Research Methods*, 39, 175–191. <https://doi.org/10.3758/BF03193146>, PubMed: 17695343
- Fernandino, L., Binder, J. R., Desai, R. H., Pendl, S. L., Humphries, C. J., Gross, W. L., et al. (2016). Concept representation reflects multimodal abstraction: A framework for embodied semantics. *Cerebral Cortex*, 26, 2018–2034. <https://doi.org/10.1093/cercor/bhv020>, PubMed: 25750259
- Goldman, N. M. (1975). The boundaries of language generation. *Paper presented at the Proceedings of the 1975 Workshop on Theoretical Issues in Natural Language Processing*. Cambridge, MA. <https://doi.org/10.3115/980190.980215>
- Hansen, T., Olkkonen, M., Walter, S., & Gegenfurtner, K. R. (2006). Memory modulates color appearance. *Nature Neuroscience*, 9, 1367–1368. <https://doi.org/10.1038/nn1794>, PubMed: 17041591
- Hayasaka, S., & Nichols, T. E. (2003). Validating cluster size inference: Random field and permutation methods. *Neuroimage*, 20, 2343–2356. <https://doi.org/10.1016/j.neuroimage.2003.08.003>, PubMed: 14683734

- Hebart, M. N., Görden, K., & Haynes, J.-D. (2015). The Decoding Toolbox (TDT): A versatile software package for multivariate analyses of functional imaging data, 8, 88. <https://doi.org/10.3389/fninf.2014.00088>, PubMed: 25610393
- Hsu, N. S., Frankland, S. M., & Thompson-Schill, S. L. (2012). Chromaticity of color perception and object color knowledge. *Neuropsychologia*, 50, 327–333. <https://doi.org/10.1016/j.neuropsychologia.2011.12.003>, PubMed: 22192637
- Hsu, N. S., Kraemer, D. J., Oliver, R. T., Schlichting, M. L., & Thompson-Schill, S. L. (2011). Color, context, and cognitive style: Variations in color knowledge retrieval as a function of task and subject variables. *Journal of Cognitive Neuroscience*, 23, 2544–2557. <https://doi.org/10.1162/jocn.2011.21619>, PubMed: 21265605
- Jackendoff, R. (1990). *Semantic structures*. Cambridge, MA: MIT Press.
- Kaiser, P. (1991). Flicker as a function of wavelength and heterochromatic flicker photometry. In F. F. Kulikowsky, V. Walsh, & I. F. Murray (Eds.), *Limits of Vision* (pp. 171–190). CRC Press.
- Klein, G. S. (1964). Semantic power measured through the interference of words with color-naming. *American Journal of Psychology*, 77, 576–588. <https://doi.org/10.2307/1420768>, PubMed: 14255565
- Kriegeskorte, N., Goebel, R., & Bandettini, P. (2006). Information-based functional brain mapping. *Proceedings of the National Academy of Sciences, U.S.A.*, 103, 3863–3868. <https://doi.org/10.1073/pnas.0600244103>, PubMed: 16537458
- Kriegeskorte, N., Mur, M., & Bandettini, P. A. (2008). Representational similarity analysis - connecting the branches of systems neuroscience. *Frontiers in Systems Neuroscience*, 2, 4. <https://doi.org/10.3389/neuro.06.004.2008>, PubMed: 19104670
- Levelt, W. J. M. (1989). *Speaking: From intention to articulation*. Cambridge, MA: MIT Press.
- Levelt, W. J. M., Roelofs, A., & Meyer, A. S. (1999). A theory of lexical access in speech production. *Behavioral and Brain Sciences*, 22, 1–38; discussion 38–75. <https://doi.org/10.1017/S0140525X99001776>, PubMed: 11301520
- Lueck, C. J., Zeki, S., Friston, K. J., Deiber, M. P., Cope, P., Cunningham, V. J., et al. (1989). The colour centre in the cerebral cortex of man. *Nature*, 340, 386–389. <https://doi.org/10.1038/340386a0>, PubMed: 2787893
- McRae, K., Cree, G. S., Seidenberg, M. S., & McNorgan, C. (2005). Semantic feature production norms for a large set of living and nonliving things. *Behavior Research Methods*, 37, 547–559. <https://doi.org/10.3758/bf03192726>, PubMed: 16629288
- Meyer, A. S., & Damian, M. F. (2007). Activation of distractor names in the picture–picture interference paradigm. *Memory & Cognition*, 35, 494–503. <https://doi.org/10.3758/BF03193289>, PubMed: 17691148
- Mitterer, H., & de Ruiter, J. P. (2008). Recalibrating color categories using world knowledge. *Psychological Science*, 19, 629–634. <https://doi.org/10.1111/j.1467-9280.2008.02133.x>, PubMed: 18727774
- Mumford, J. A. (n.d.). Efficiency day 3: MATLAB example. Retrieved from <https://www.youtube.com/channel/UCZ7gF0zm35FwrFpDND6DWaA/featured>
- Mumford, J. A., Davis, T., & Poldrack, R. A. (2014). The impact of study design on pattern estimation for single-trial multivariate pattern analysis. *Neuroimage*, 103, 130–138. <https://doi.org/10.1016/j.neuroimage.2014.09.026>, PubMed: 25241907
- Mumford, J. A., Turner, B. O., Ashby, F. G., & Poldrack, R. A. (2012). Deconvolving BOLD activation in event-related designs for multivoxel pattern classification analyses. *Neuroimage*, 59, 2636–2643. <https://doi.org/10.1016/j.neuroimage.2011.08.076>, PubMed: 21924359
- Nelson, D. L., McEvoy, C. L., & Schreiber, T. A. (2004). The University of South Florida free association, rhyme, and word fragment norms. *Behavior Research Methods, Instruments, & Computers*, 36, 402–407. <https://doi.org/10.3758/BF03195588>, PubMed: 15641430
- Nichols, T., Brett, M., Andersson, J., Wager, T., & Poline, J. B. (2005). Valid conjunction inference with the minimum statistic. *Neuroimage*, 25, 653–660. <https://doi.org/10.1016/j.neuroimage.2004.12.005>, PubMed: 15808966
- Nili, H., Wingfield, C., Walther, A., Su, L., Marslen-Wilson, W., & Kriegeskorte, N. (2014). A toolbox for representational similarity analysis. *PLoS Computational Biology*, 10, e1003553. <https://doi.org/10.1371/journal.pcbi.1003553>, PubMed: 24743308
- Parkes, L. M., Marsman, J.-B. C., Oxley, D. C., Goulermas, J. Y., & Wuerger, S. M. (2009). Multivoxel fMRI analysis of color tuning in human primary visual cortex. *Journal of Vision*, 9, 1–13. <https://doi.org/10.1167/9.1.1>, PubMed: 19271871
- Poser, B. A., Versluis, M. J., Hoogduin, J. M., & Norris, D. G. (2006). BOLD contrast sensitivity enhancement and artifact reduction with multiecho EPI: Parallel-acquired inhomogeneity-desensitized fMRI. *Magnetic Resonance in Medicine*, 55, 1227–1235. <https://doi.org/10.1002/mrm.20900>, PubMed: 16680688
- Redmann, A., FitzPatrick, I., Hellwig, F., & Indefrey, P. (2014). The use of conceptual components in language production: An ERP study. *Frontiers in Psychology*, 5, 363. <https://doi.org/10.3389/fpsyg.2014.00363>, PubMed: 24808878
- Redmann, A., FitzPatrick, I., & Indefrey, P. (2019). The time course of colour congruency effects in picture naming. *Acta Psychologica*, 196, 96–108. <https://doi.org/10.1016/j.actpsy.2019.04.005>, PubMed: 31005782
- Roelofs, A. (1992). A spreading-activation theory of lemma retrieval in speaking. *Cognition*, 42, 107–142. [https://doi.org/10.1016/0010-0277\(92\)90041-F](https://doi.org/10.1016/0010-0277(92)90041-F), PubMed: 1582154
- Roelofs, A. (1993). Testing a non-decompositional theory of lemma retrieval in speaking: Retrieval of verbs. *Cognition*, 47, 59–87. [https://doi.org/10.1016/0010-0277\(93\)90062-Z](https://doi.org/10.1016/0010-0277(93)90062-Z), PubMed: 8482071
- Roelofs, A. (1997). A case for nondecomposition in conceptually driven word retrieval. *Journal of Psycholinguistic Research*, 26, 33–67. <https://doi.org/10.1023/A:1025060104569>
- Scheibe, K., Shaver, P. R., & Carrier, S. C. (1967). Color association values and response interference on variants of the Stroop test. *Acta Psychologica*, 26, 286–295. [https://doi.org/10.1016/0001-6918\(67\)90028-5](https://doi.org/10.1016/0001-6918(67)90028-5), PubMed: 5582591
- Seymour, K., Clifford, C. W. G., Logothetis, N. K., & Bartels, A. (2009). Coding and binding of color and form in visual cortex. *Cerebral Cortex*, 20, 1946–1954. <https://doi.org/10.1093/cercor/bhp265>, PubMed: 20019147
- Seymour, K., Clifford, C. W., Logothetis, N. K., & Bartels, A. (2010). Coding and binding of color and form in visual cortex. *Cerebral Cortex*, 20, 1946–1954. <https://doi.org/10.1093/cercor/bhp265>, PubMed: 20019147
- Seymour, K., Williams, M. A., & Rich, A. N. (2015). The representation of color across the human visual cortex: Distinguishing chromatic signals contributing to object form versus surface color. *Cerebral Cortex*, 26, 1997–2005. <https://doi.org/10.1093/cercor/bhv021>, PubMed: 25681421
- Simmons, W. K., Ramjee, V., Beauchamp, M. S., McRae, K., Martin, A., & Barsalou, L. W. (2007). A common neural substrate for perceiving and knowing about color. *Neuropsychologia*, 45, 2802–2810. <https://doi.org/10.1016/j.neuropsychologia.2007.05.002>, PubMed: 17575989
- Tanaka, J. W., & Presnell, L. M. (1999). Color diagnosticity in object recognition. *Perception & Psychophysics*, 61, 1140–1153. <https://doi.org/10.3758/bf03207619>, PubMed: 10497433
- Vandenbroucke, A. R. E., Fahrenfort, J. J., Meuwese, J. D. I., Scholte, H. S., & Lamme, V. A. F. (2016). Prior knowledge

- about objects determines neural color representation in human visual cortex. *Cerebral Cortex*, *26*, 1401–1408. <https://doi.org/10.1093/cercor/bhu224>, PubMed: 25323417
- van Leeuwen, T. M., Petersson, K. M., & Hagoort, P. (2010). Synaesthetic colour in the brain: Beyond colour areas. A functional magnetic resonance imaging study of synaesthetes and matched controls. *PLoS One*, *5*, e12074. <https://doi.org/10.1371/journal.pone.0012074>, PubMed: 20711467
- Verhagen, L., Dijkerman, H. C., Grol, M. J., & Toni, I. (2008). Perceptuo-motor interactions during Prehension movements. *Journal of Neuroscience*, *28*, 4726–4735. <https://doi.org/10.1523/JNEUROSCI.0057-08.2008>, PubMed: 18448649
- Zeki, S. (1983). Colour coding in the cerebral cortex: The responses of wavelength-selective and colour-coded cells in monkey visual cortex to changes in wavelength composition. *Neuroscience*, *9*, 767–781. [https://doi.org/10.1016/0306-4522\(83\)90266-x](https://doi.org/10.1016/0306-4522(83)90266-x), PubMed: 6621878
- Zeki, S. (1993). *A vision of the brain*. Cambridge, MA: Blackwell Scientific Publications.
- Zeki, S., & Marini, L. (1998). Three cortical stages of colour processing in the human brain. *Brain: A Journal of Neurology*, *121*, 1669–1685. <https://doi.org/10.1093/brain/121.9.1669>, PubMed: 9762956
- Zeki, S., Watson, J. D., Lueck, C. J., Friston, K. J., Kennard, C., & Frackowiak, R. S. (1991). A direct demonstration of functional specialization in human visual cortex. *Journal of Neuroscience*, *11*, 641–649. <https://doi.org/10.1523/jneurosci.11-03-00641.1991>, PubMed: 2002358